



Improvement of sandy soil to prevent hydraulic failure using BCF fibers and geotextiles

Shayan Ghasemian Langroudi¹ · Amirali Zad¹ · Ali M. Rajabi²

Received: 28 January 2021 / Accepted: 14 July 2021 / Published online: 5 August 2021
© Saudi Society for Geosciences 2021

Abstract

Sand boiling is a type of hydraulic failure occurring the downstream of dams with huge damages. In this study, the reinforcement effect of Firuzkuh sand with bulk continuous filament (BCF) fibers and geotextile (woven and nonwoven) on the resistance to boiling is examined on a laboratory scale. For this purpose, an upward seepage apparatus was designed and fabricated. In reinforcement with BCF fibers, with increasing the weight percentage of fibers, soil strength increased and the permeability coefficient was changed. In soil reinforcement with geotextile, two types of woven and nonwoven geotextiles were used in two modes of one and two layers. Based on the results of the performed tests on these samples, the reinforced samples have shown more resistance to boiling than the natural samples. Also, the increase in critical hydraulic gradient and seepage force (to sand boiling) was found to be a function of the type and number of geotextile layers. Moreover, in this research, the effect of the relative compaction of the sample on permeability and critical hydraulic gradient of samples (reinforced and unreinforced) was investigated. According to the results, in denser samples, the boiling is delayed and soil improvement (a reinforcement with fibers and geotextile) is significantly effective.

Keywords Geosynthetics · Hydraulic failure · Sand boiling · Critical hydraulic gradient · Soil reinforcement · BCF fibers and geotextile

Introduction

Sand boiling and piping are phenomena that occur inside the porous soil mass due to upward water seepage. According to the Mohr-Coulomb failure criterion for granular soils, the shear strength in sandy soils dissipates with zero effective stress and due to the lack of cohesion between the particles, the soil collapses. Moreover, according to Bernoulli's

Equation in fluid mechanics, the head difference between two points causes water movement from a point with a higher potential to a point with a lower potential. Moving water by applying hydrodynamic forces to soil particles can decrease or increase the effective stress of soil. As the upward water moves, the effective stress decreases, and the seepage force is applied to the soil particles in the form of erosive and uplifting. In other words, the resistance and driving factors in the sand boiling and piping phenomenon are the effective stress between the particles and the seepage force. In this situation, if the driving factor overcomes the resistant factor and the effective stress decreases to zero, hydraulic failure occurs and the sand boils. Terzaghi (1943) implemented a series of theoretical and laboratory investigations and then proposed Eq. (1) as the boundary condition for the occurrence of the sand boiling and piping phenomenon (i_{cr}).

$$i_{cr} = \frac{G_s - 1}{e + 1} \quad (1)$$

where G_s is the specific gravity of the soil and e is the void ratio. Based on this equation, in unreinforced soils (without the use of reinforcing elements), the amount of critical

Responsible Editor: Broder J. Merkel

✉ Amirali Zad
a.zad@iauctb.ac.ir

Shayan Ghasemian Langroudi
Shayanghasemian3@gmail.com

Ali M. Rajabi
amrajabi@ut.ac.ir; amrajabi@ymail.com

¹ Faculty of Civil and Earth Resources Engineering, Islamic Azad University, Central Tehran branch, Tehran, Iran

² Engineering Geology Department, School of Geology, University of Tehran, Tehran, Iran

hydraulic gradient of sand increases with increasing relative compaction of soil (reducing void ratio), and sand boiling is delayed. To determine the critical hydraulic gradient of the soils, Wu (1980); Liu (1992); and Zhou et al. (2010) provided theoretical relationships to predict the occurrence of the piping phenomenon for hydraulic structure. Piping is the progressive erosion and transportation of soil particles along a flow path (Falamaki et al. 2020). There is a possibility of hydraulic fracture at the downstream of the dams and hydraulic dikes which this failure in the form of sand boiling or piping leads to the total or partial failure of these structures. Foster et al. (2000) conducted comprehensive studies on the causes of dam failure until 1986 and stated that 46% of all failures in dams are attributed to the piping occurrence in the embankment or foundation of dams. However, it is of note that piping is most common in fine-grained soils such as fine sand, silt, and coarse clay (Bhagyalekshmi et al. 2015).

Skempton and Brogan (1994) designed and fabricated an apparatus to simulate the sand boiling and piping phenomenon. Next, they conducted a laboratory study on sandy gravel soils and examined the relation of critical hydraulic gradient and stability index of soil. The basis of this apparatus is to create a head difference between the lower and upper points of the soil sample and to create an upward flow in the soil. Furumoto et al. (2002); Sivakumar and Vasudevan (2008); Das et al. (2009); Das and Viswanadham (2010); Soltannejad et al. (2016); Estabragh et al. (2016); and Yang et al. (2017) examined the effect of sandy soil reinforcement with natural and synthetic fibers on the critical hydraulic gradient. The results of these researches showed that reinforced soil with randomly distributed fibers is more resistant than natural soil samples. In these studies, parameters such as the type, length, and percentage of fibers mixing were evaluated. In general, the results of these studies show that with increasing the weight percentage and length of the fiber, the resistance of the samples against the piping is increased. Richards and Reddy (2010) investigated the critical hydraulic gradient of the soil and the discharge velocity during the piping for noncohesive soils. Van Beek et al. (2010), based on the Sellmeijer model (Sellmeijer 1988), examined the piping process at small, medium, and large scales for water retaining structure in the Netherlands. Next, based on their observations, they introduced four phases of seepage, backward erosion, widening of pipe, and final fracture of the levee for the occurrence of piping. Fujisawa et al. (2013) conducted laboratory and numerical studies and obtained the seepage force and velocity of particle movement during sand boiling. Yang and Wang (2017) performed statistical comparisons between theoretical relationships and laboratory results of hydraulic failure. Next, by calculating and measuring critical hydraulic gradient, they obtained the margin of these relationships error compared to laboratory observations. Divya et al. (2018) examined the effect of polypropylene

and polyethylene fibers on the permeability of two types of silty soils and stated that increasing the characteristics such as percentage and length of fibers in silty soil reinforcement causes variation in the permeability coefficient of the sample, leading to some changes in the water seepage velocity. Chegenizadeh et al. (2018) performed a cyclic triaxial test on reinforced silty soil with fibers (BCF) and compared the results for natural and reinforced specimens. They found that the number of required cycles for the occurrence of liquefaction in reinforced samples is higher than unreinforced specimens. Taghvaei et al. (2019) performed a numerical study at upstream of the dam to reduce seepage from the body of a homogeneous earth dam. In this research, they examined the effect of mixed sandy soil blanket using different weight percentages of montmorillonite nano-clay. Yang et al. (2019) conducted a case study of the Mawujing tailing dam in China and based on their statistical and dynamic analysis, they considered the use of nonwoven geotextile tubes as a suitable alternative for fine materials in the design and operation phase of the dam. Azar et al. (2019) investigated the process of sand boiling phenomenon occurrence in the foundation of hydraulic structures by numerical modeling. According to their results, in addition to the parameters in the proposed equation by Terzaghi (1943), to determine the critical hydraulic gradient of soil, other factors such as dilation angle and internal friction angle of sand also can affect the safety and stability of soils against sand boiling. Jewel et al. (2019) performed sand boiling test on silica sand and reported that the cause of sand boiling is zero shear stress of cohesionless soils and concluded that there is a linear relationship between critical shear stress and hydraulic gradients and evaluated the trend of shear stress variations as a decrease in upward seepage. Tian et al. (2020) by investigating the hydraulic failure of the erosion type found that coarse particles suspended in a fine matrix could somewhat increase the soil's shear strength and reduce its internal erodibility.

Reviewing previous studies on seepage and hydraulic failure reveals that the majority focus of the past researches have been on soil reinforcement with fibers, and the effect of percentages and lengths of different types of fibers on sandy soils with different amounts of silt has been investigated. Reviewing these studies shows that due to the need to maintain hydraulic structures, the issue of soil improvement against hydraulic failures such as sand boiling is still an important challenge for geotechnical engineers. In the present study, BCF yarn and geotextile (both nonwoven and woven) were used as reinforcing elements for Firuzkuh 171 sandy soil (located in the north of Iran) and the effect of fiber percentage, relative compaction, type, and the number of geotextile layers on the critical hydraulic gradient of the sand was investigated. To the best of our knowledge, past research has been limited to three types of polyethylene, polyester, and polypropylene

fibers and the effect of parameters such as relative density and relative compaction of the sample on critical hydraulic gradients of the sample has been less studied. Therefore, the type of used reinforcement (BCF fibers and geotextile) in this research and the construction of the sample with different compression levels have not been investigated so far. Also, the use of BCF fibers in this study, regarding their applications in carpets and rugs, is a suitable and environmentally friendly option that can be used as a recyclable material for soil reinforcement.

Materials and methods

In this study, Firuzkuh 171 sand (standard sand in the north of Iran), BCF fibers, woven, and nonwoven geotextiles were used as reinforcement elements. Firuzkuh sands are extracted from the quarry of Firuzkuh city, located in the north of Iran and using crushers and screening in different types, they are used for various purposes such as water purification and casting. Since Firuzkuh 171 sand lacks fines (silt and clay), it has a high potential for boiling and piping. In order to determine the physical and mechanical properties of the soil, BCF fibers, and geotextiles which have been used in this research, identification tests have been performed.

Soil characteristics

As mentioned earlier, the soil used in this study is sandy soil with zero fine-grained (passing through sieve No. 200) percentage and all soil particles being smaller than 1 mm. The obtained values of the uniformity coefficient and the curvature coefficient from the sieve analysis for this soil are 2.2 and 1.06, respectively. According to the unified classification system (ASTM D2487-17 (2017)), the studied soil is named SP (poorly graded sand). To determine the maximum and minimum dry unit weight of soil, a relative density test (ASTM D4253-16e1 (2016) & ASTM D4254-16 (2016)) was carried out. To make and prepare the samples in the loose and dense state, sand vibration along with surcharge load and sand pluviation methods was used, respectively. Based on these tests, the minimum and maximum void ratios of this sand are 0.586 and 0.984, respectively. Table 1 shows the soil properties in this study.

Reinforcement specifications

The used reinforcements in this study include BCF fibers (in the form of mixing with randomly distributed) and geotextiles (in two modes of woven and nonwoven) (Figure 1). BCF reinforcement is in the form of yarn that is obtained from the weaving of polyester and polypropylene microfibers and is used in the industry for weaving carpets, rugs, and other loom

Table 1 Physical and mechanical properties of the soil

Property	Value
Maximum dry unit weight (g/cm^3)	1.67
Minimum dry unit weight (g/cm^3)	1.36
Specific gravity (G_s)	2.65
Gravel percent (%)	0
Sand percent (%)	100
Silt percent (%)	0
D10 (mm)	0.17
D50 (mm)	0.36

textiles. In this research, the number of filaments and deniers of these fibers are 400 and 900, respectively, and the length of each filament is 5 cm. Another type of used reinforcements in this study is woven and nonwoven geotextiles (both are made of polyester) and their main difference is in the rate of water permeability. Tables 2 and 3 show the physical and mechanical properties of BCF yarn and geotextiles, respectively.

The sand boiling test device

In general, there are no specific standards and criteria for sand boiling and piping modeling device. The idea of piping device design was first proposed by Skempton and Brogan (1994). Other researchers, such as Furumoto et al. (2002); Sivakumar and Vasudevan (2008); Das et al. (2009); Das and Viswanadham (2010); Soltannejad et al. (2016); and Estabragh et al. (2016), designed devices using the Skempton and Brogan (1994) model to determine critical hydraulic gradients. In this study, using the concept of sand boiling and piping phenomenon, a specific device has been made to simulate this phenomenon. Figures 2 and 3 show the details of the device in the form of schematically and realistically, respectively. According to Figure 2, the device consists of an elevator with a range (maximum height that the moving plate can climb) of 80 cm and has a moving plate and a platform (fixed plate).

A moving plate is mounted on the right side of the device, on which the water supply reservoir is placed. This reservoir is Teflon cylindrical with an inner diameter of 10 cm, and the water level control pipe (2) is installed at a distance of 10 cm

Table 2 Physical and mechanical properties of BCF fiber

Property	Value
Ultimate tensile strength (Mpa)	481
Elastic modulus (Gpa)	3.43
Specific gravity	1.33
No. of denier	2.5
type	Polyester

Table 3 Physical and mechanical properties of geotextiles

Material name	Geotextile type	Permeability (cm/s)	Tensile strength (N)	Opening size (mm)	Thickness (mm)
Woven	Polyester	0.01	1250	0.07	Less than 1
Nonwoven	Polyester	0.24	700	0.21	1

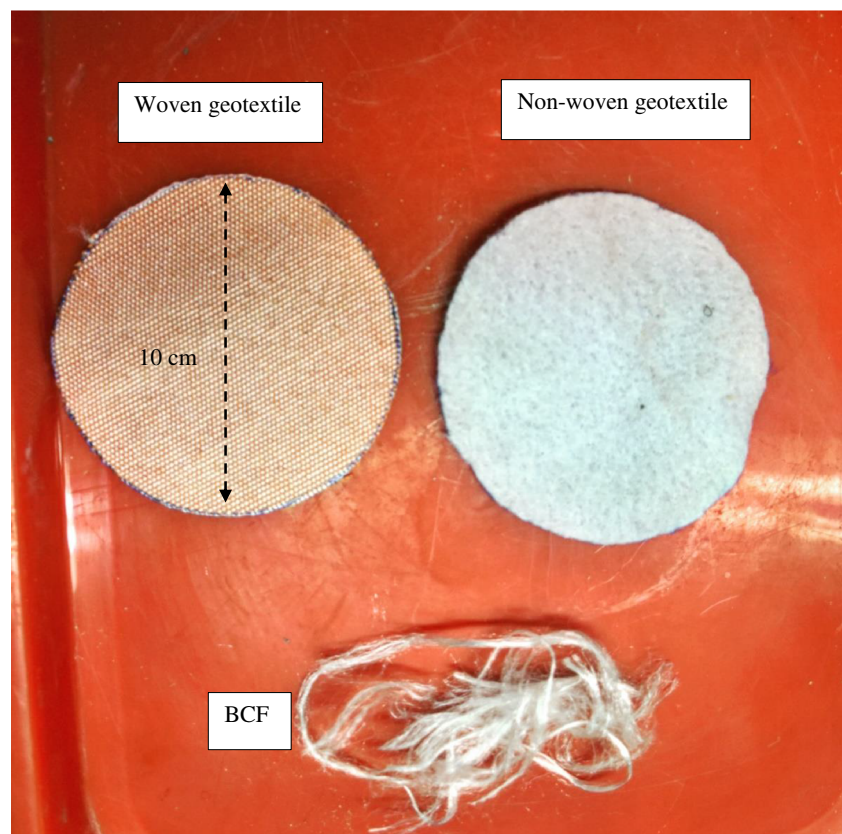
from the reservoir base. In other words, excess water is removed from the system through the water level control pipe and the reservoir can hold water up to a height of 10 cm. As shown in Figure 2, on the left side of the device, there is a platform (fixed plate) which a calm reservoir, a sample cell, and a downstream transparent ring are placed on it. The calm reservoir is connected to the water supply reservoir by the water flow transfer tube (3) and the cell (sample location) is installed on it. The sample cell is a Teflon cylinder with a diameter and height of 10 cm. The calm reservoir leads to the uniform distribution of the inlet water pressure at the base of the sample cell. In the connection path of the water transfer tube, a valve (cut off/on) has been installed, so that the increasing process of the water height in the upstream area of the system can be performed step by step. To measure the hydraulic gradient, two piezometers (4) with an inner diameter of 4 mm and a distance of 7.5 cm from each other were used in the bottom and top of the sample. At the bottom of the sample cell, there is a screen (number 200) to keep the soil in place and allow water to enter the sample cell which causes the

uniform distribution of water pressure and prevents soil particles fall inside the calm reservoir. On the sample cell, a transparent ring was used to see the heaving of the soil surface during boiling, so that the water outlet tube (to exit the water from the system and to measure the discharge flow) is placed at a distance of 2.5 cm from the sample surface. In this device, the elevation of the water level control pipe and the water outlet pipe show the water level in the upstream and downstream of the system, respectively, and the zero-gradient point (alignment line) is defined as the alignment of the upstream and downstream height. Also, due to the maximum range of elevators and 10-cm height of the sample cell, the device can apply the hydraulic gradient up to a value of 8 on the sample.

Method of sand boiling tests

Sample preparation

As was mentioned earlier, in this study, the soil is reinforced with BCF fiber, woven, and nonwoven geotextiles. In the

Fig. 1 Geotextiles and BCF fibers

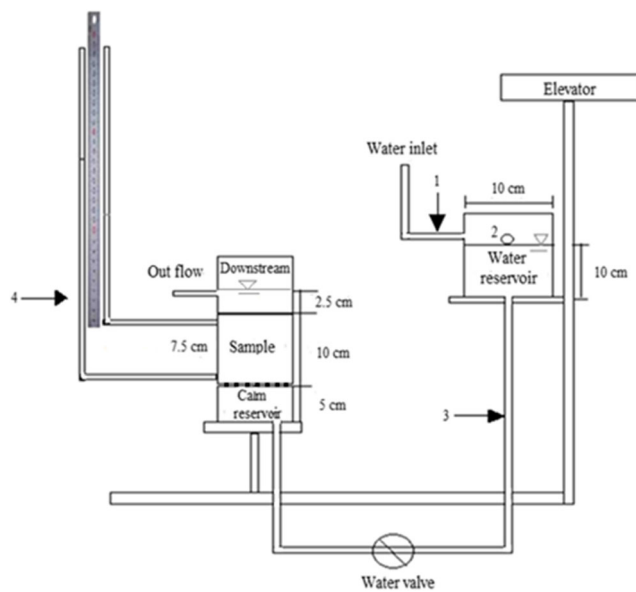


Fig. 2 Schematic of the sand boiling test device (upward seepage test system): (1) water supply pipe, (2) water level control pipe, (3) water flow transfer tube, and (4) piezometer

reinforcement with fiber, three different weight percentages of 0.1, 0.25, and 0.5 were used and in the reinforcement with geotextiles (woven and nonwoven), the reinforcement elements are used as single-layer and double-layer. Besides, natural and reinforced specimens were made in three loose, medium, and dense compaction states at 80%, 90%, and 96% relative compactions, respectively. To make the samples with different compaction status, due to the sandy nature of the studied soil, the vibration method with applying overhead has been used to obtain the maximum dry unit weight of the sample that the frequency and amplitude of vibration according to the standard (ASTM D4253-16) are 2600 rpm and 0.635 cm, correspondingly. The compaction conditions of reinforced specimens with geotextile do not differ with the natural specimens in terms of maximum dry unit weight, because there is no mixing between soil particles and geotextile tissue, and geotextiles are placed as a layer at different distances within the soil. While the random distribution of fibers inside the soil affects the maximum dry unit weight sample. For this purpose, the test of determining the maximum dry unit weight

Fig. 3 Overview of upward seepage device

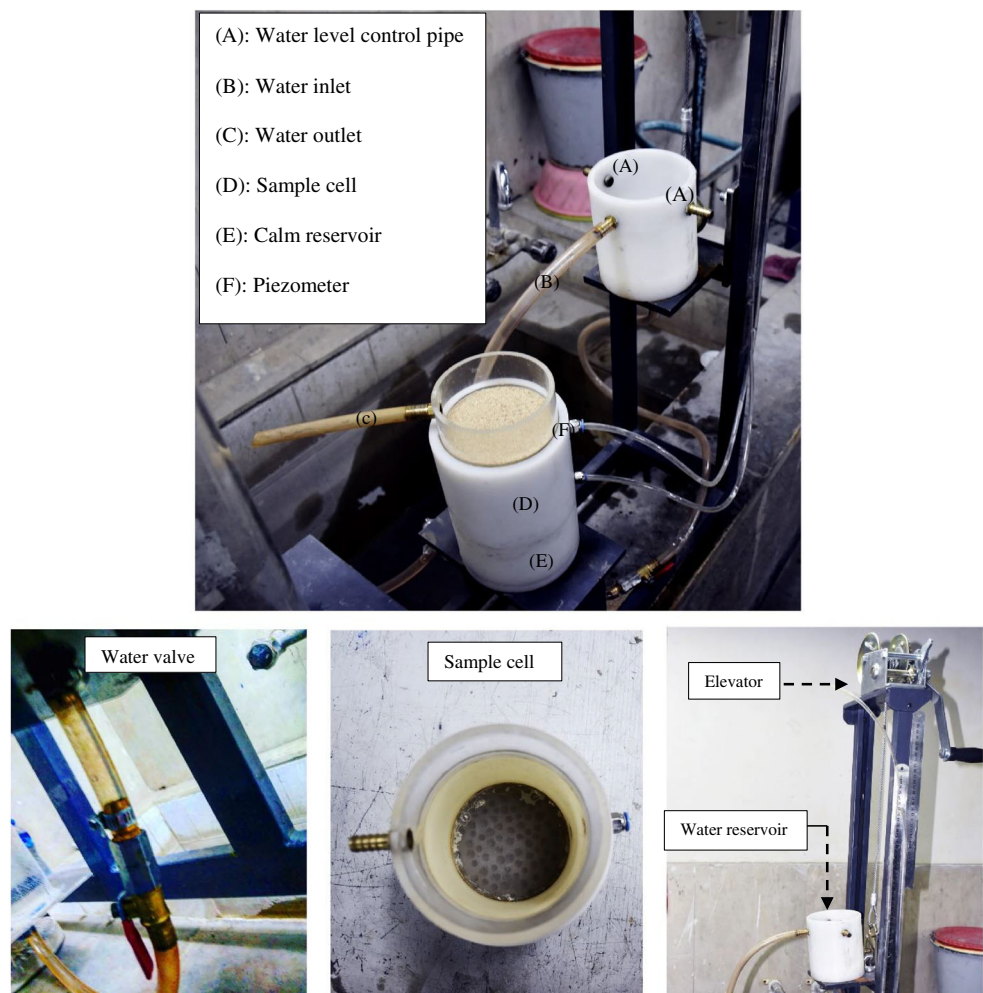


Table 4 Maximum dry unit weight of the samples

Fiber content (%)	Length of fiber (cm)	Maximum dry unit weight (g/cm ³)
0.00	5	1.67
0.10	5	1.62
0.25	5	1.61
0.50	5	1.59

was performed on a natural and reinforced sample with a weight percentage of 0.1, 0.25, and 0.5 (Table 4 and Figure 4).

According to Figure 4, the maximum dry unit weight of natural soil is 1.67 (g/cm³). However, with the addition of fibers due to the replacement of fibers with soil particles (fiber density is lower than soil particles), the maximum dry unit weight of the sample is reduced. So that, by adding 0.5% fibers to the soil, the maximum dry unit weight of the sample is reduced to 1.59 g/cm³. In this study, the concept of relative density has been used to determine the dry specific weight of samples in different compaction conditions. For this purpose, the relative compaction for the three states of loose, medium, and dense samples is considered 80%, 90%, and 96%, respectively. According to Eq. (2), the dry unit weight of the sample (γ_{sample}) with relative compaction of R_c is as follows:

$$\gamma_{\text{sample}} = R_c \gamma_{d\text{max}} \quad (2)$$

where $\gamma_{d\text{max}}$ is the maximum dry unit weight of soil. Accordingly, the weight value of the natural sample of W_s inside the cell of the device can be calculated by having the sample volume (V) (Eq. 3):

$$W_s = \gamma_{\text{sample}} V \quad (3)$$

As mentioned earlier, reinforcement with geotextiles is considered as one and two layers. In the single-layer case, the geotextiles are located in the center of the cell (i.e., at a distance of $h/2$ from the sample cell base (h is the height of the device cell) and in the two-layer mode, the distance between the

geotextiles is $h/3$ (Figure 5). To determine the weight of the required soil to make reinforced specimens with geotextile, the dry unit weight of the natural sample is used. Consequently, for reinforced samples with one and two layers of geotextiles, the weight amount of the desired soil is divided into two and three equal parts, respectively and geotextiles are layered on the soil.

To obtain the soil weight (W_s) and the weight of the used fibers (W_f) for reinforced samples with $F\%$ fibers and the relative compaction of R_c , Eqs. (5) and (6) are used:

$$W_T = R_c \gamma_{d\text{max}} (F\%) V \quad (4)$$

$$W_s = \frac{W_T}{1 + F} \quad (5)$$

$$W_f = F W_s \quad (6)$$

In these relations, $\gamma_{d\text{max}} (F\%)$ is the maximum dry unit weight of the sample with $F\%$ fibers and W_T is the weight of the reinforced sample with fibers. Accordingly, reinforced samples by fiber are made in different mixing percentages and various compaction conditions.

How to perform the boiling test

To perform the sand boiling test, in the first step, the sample is compacted to a certain extent using a plastic hammer and tamper (Figure 6). The mixing of fiber with sand has been done with the proposed method by Yetimoglu and Salbas (2003) for reinforced specimens by fibers. For this purpose, the weight of

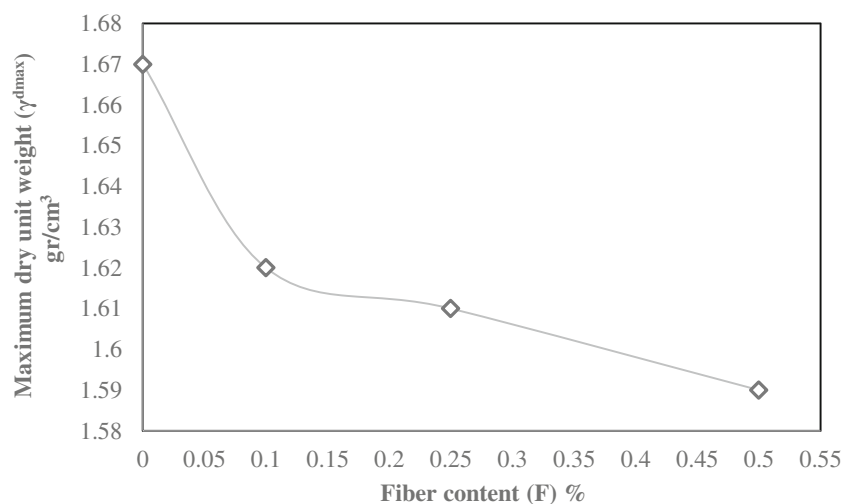
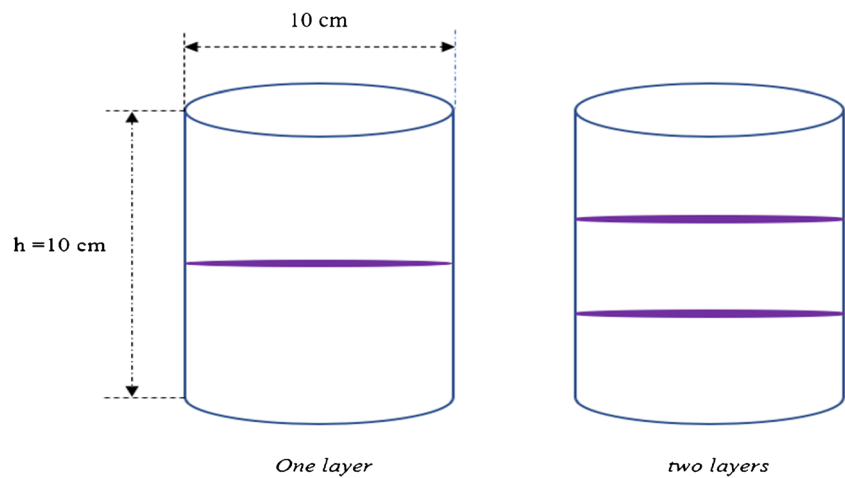
Fig. 4 Variation of maximum dry unit weight with different fiber contents

Fig. 5 Location of the geotextile's layers in the cell of the sand boiling apparatus



soil and fibers for each sample with a certain percentage of fibers is calculated according to the volume of the device mold and the relative compaction of the sample. Then, the amount of soil and fibers are divided into three almost equal parts and in each part, the fibers and soil are mixed together so that the distribution of fibers in the soil is almost uniform. After preparing the samples, the sample cell is placed on the calm reservoir.

To prevent the bubble formation inside the empty space of the calm reservoir and the uniform distribution of water pressure, the calm reservoir is filled with rubble. After placing the sample cell on the calm reservoir, the water supply reservoir is placed 2cm above the alignment line of upstream with downstream. Afterward, the valve (cut off/on) is opened to allow water to flow from the reservoir to the sample cell. The saturation time of the samples depends on the permeability coefficient of the sample. The condition for the saturation and stability of the flow is a constant outflow. After saturation of the sample, the output discharge rate can be calculated using the output water volume and a timer. Finally, the discharge velocity (v) of the flow is obtained from Eq. (7).

$$v = \frac{Q}{A} \tag{7}$$

where Q and A are the flow rate and sample cross-section, respectively. Hydraulic gradients can also be calculated using the measured differences head by piezometers. After recording the discharge velocity and hydraulic gradient, the flow valve is closed and the elevator is placed at a higher level (about 2 cm higher than the previous step). Then, the flow valve is reopened and after stabilizing the water flow, the water flow velocity and hydraulic gradient are measured as the previous step. This process is performed in each hydraulic gradient to determine related discharge velocity for different hydraulic heads (different heights of the water supply reservoir). The water supply reservoir rises to the point where the boiling is observed and after that, the test is finished. At the moment of boiling, the sand particles are separated from the soil texture, and by moving upward causes the hydraulic failure of the sample. In this study, conditions such as sand boiling, heaving surface of the sample, muddy water at the downstream of the system, and increase in flow discharge are considered as signs of hydraulic failure. If one or more of these conditions are observed, the test is completed and the water flow velocity diagram to the hydraulic gradient of the sample is plotted. Using this diagram, the values of the critical hydraulic gradient, the resistant force to the boiling

Fig. 6 (a) Sample compaction method and (b) from right to left respectively: tamper, calm reservoir, and sample cell

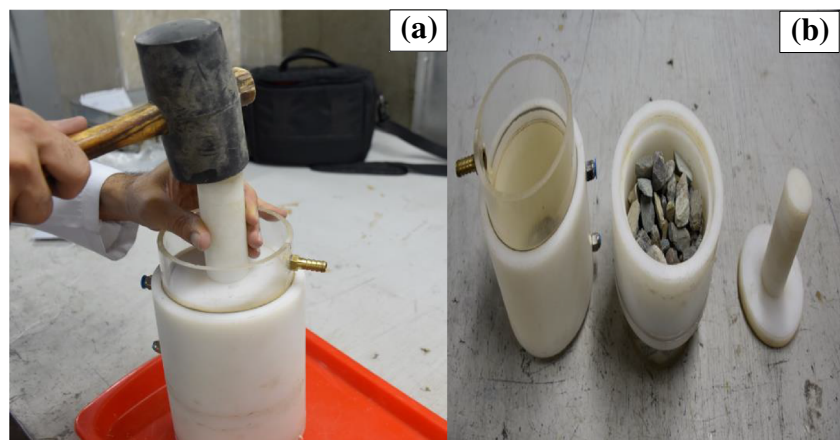
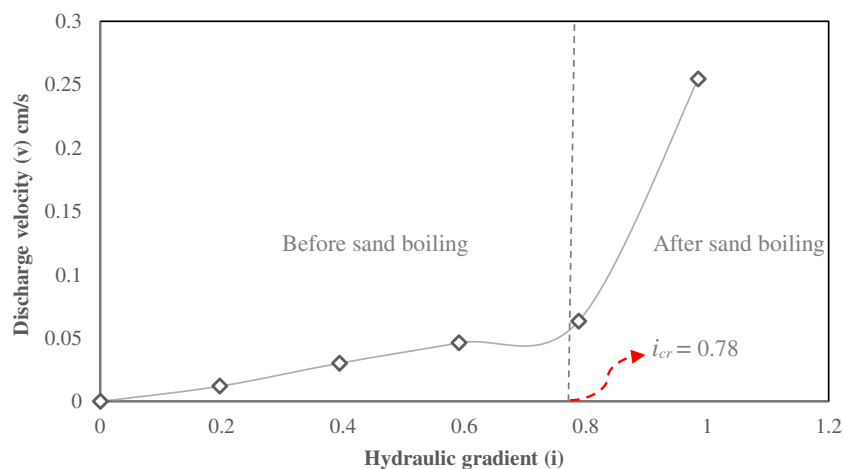


Fig. 7 Diagram of the water discharge velocity against hydraulic gradient for natural sample ($R_C = 80\%$)



phenomenon, the permeability coefficient, and the flow mode (turbulent and laminar flow) are obtained. In this study following Darcy's law, to calculate the permeability coefficient of the samples, from ratios average of discharge velocity to hydraulic gradient for different points of this graph ($v-i$) have been used that the Reynolds number of this point must be less than 1 (the laminar flow) (Das 2019). Figure 7 shows the water discharge velocity to the hydraulic gradient of the natural sample with relative compaction of 80%. According to this figure, the intersection of the passing vertical line through the fracture point with the axis of the hydraulic gradient represents the critical hydraulic gradient. This line divides the graph into two parts before and after boiling. For the used sandy soil in this study, Darcy's law is valid for all points in

the pre-boiling stage, while after the occurrence of sand boiling, turbulence flow is observed.

The Reynolds number criterion for determining the flow mode in different references is provided only for unreinforced samples. As a result, for natural samples at relative compaction of 80%, 90, and 96% (for loose, medium compaction, and dense samples, respectively), the Reynolds number values for hydraulic gradients before and after the boiling phenomenon have been calculated (pre-boiling points are dots where their hydraulic gradient is less than i_{cr}). By examining the used soil in this investigation, the flow mode changed from calm to turbulent at the moment of boiling, and the soil resistance against seepage was eliminated and as a result, the soil has failed. Figure 8

Fig. 8 The situation of the samples during sand boiling: (a) and (b) laminar flow (before boiling); (c) and (d) turbulent flow (after boiling)

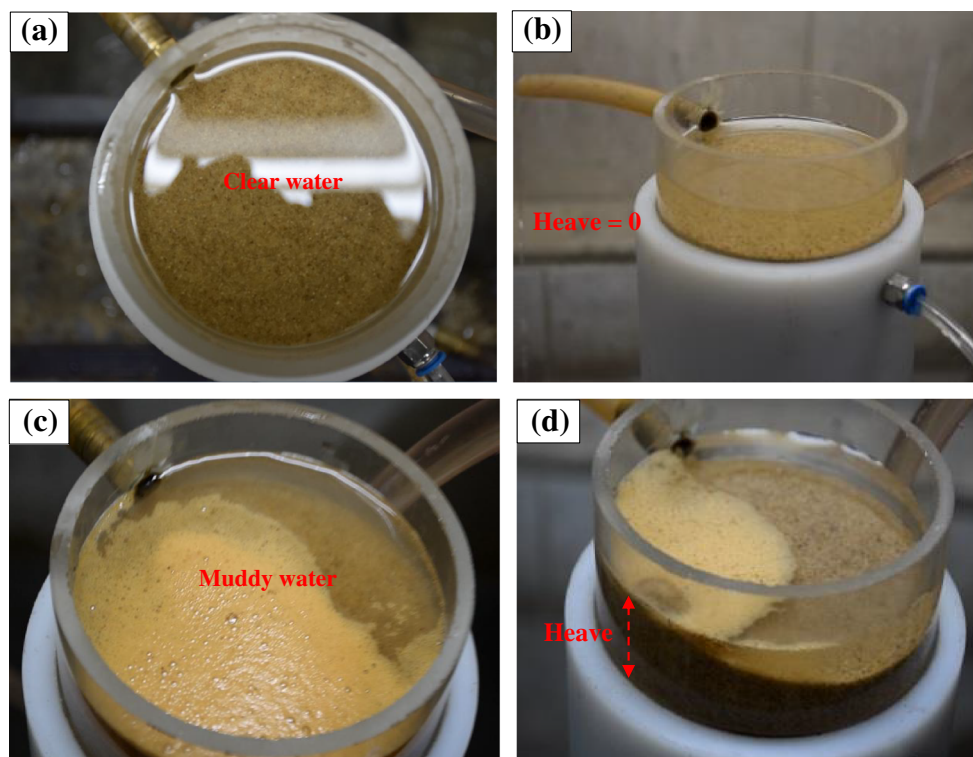


Table 5 Details of boiling test results for the sand reinforced by BCF

Fiber content (%)	Relative compaction (%)	i_{cr}	k (cm/s)	Reynolds number (before sand boiling)	Reynolds number (after sand boiling)	Seepage force during sand boiling (N)
0	80	0.78	0.078	0.228	1.46	6.12
0	90	0.98	0.055	0.206	1.26	7.69
0	96	1.50	0.030	0.213	1.80	11.77
0.1	80	0.98	0.084			7.69
0.1	90	1.28	0.054			10.04
0.1	96	2.16	0.029			17.01
0.25	80	0.98	0.095			7.693
0.25	90	1.57	0.053			12.32
0.25	96	2.56	0.028			20.09
0.5	80	0.98	0.132			7.69
0.5	90	1.67	0.048			13.10
0.5	96	3.05	0.024			23.94

The Reynolds number is estimated using $R_e = \frac{vD\rho}{\mu}$ (Das 2019)

shows the situation of the sample in the laminar and turbulent modes.

As shown in Figure 8c and d, the sample heave occurred at the moment of boiling and as a result, the sand particles moved upwards and the sample’s resistance disappeared against seepage and finally with the sudden failure of the sample, the flow discharge increases. The seepage force (p_w) at the moment of boiling is calculated from Eq. (8).

$$p_w = \gamma_w i_{cr} V \tag{8}$$

where γ_w , i_{cr} , and V are the specific weight of water, critical hydraulic gradient, and sample volume inside the device, respectively.

Results and discussion

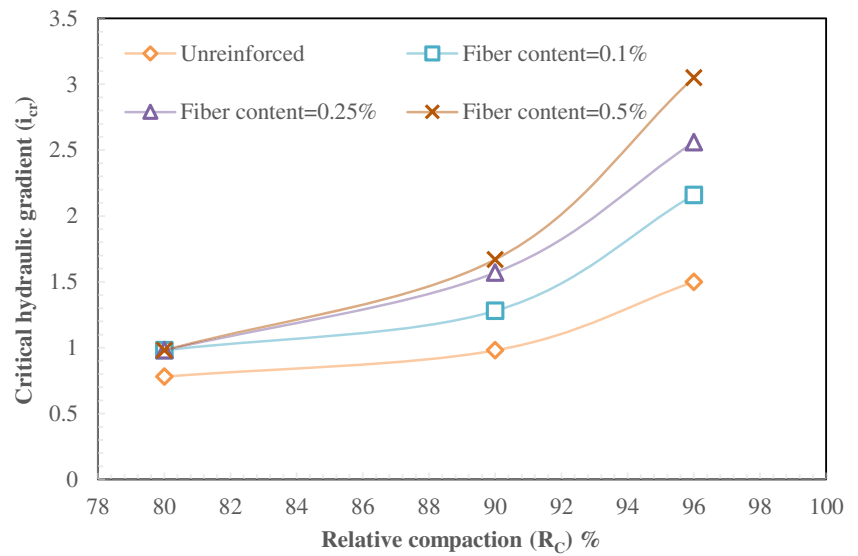
In this study, considering three compaction states loose, medium density, and dense for all samples (natural and reinforced), 24 sand boiling experiments were performed on the samples. The tested samples include natural, fiber-reinforced samples at mixing percentages of 0.1, 0.25, and 0.5 and as well as reinforcement with woven and nonwoven geotextiles in two modes of single and double layers. The results of sand boiling tests for natural and reinforced samples with fiber and geotextiles (including permeability coefficient, critical hydraulic gradient, and seepage force at the time of boiling) are presented in Tables 5 and 6, respectively.

Table 5 shows that amounts of the Reynolds numbers are calculated for natural samples at the after and before boiling points. Accordingly, for natural samples, the Reynolds number before the boiling point for all three samples is less than 1 and indicates a laminar flow. The laminar flow is the zone for determining the permeability coefficient because Darcy’s law is valid for this situation. The number of Reynolds points after boiling for natural samples is higher than 1 and represents a turbulent flow. In other words, with hydraulic failure in the samples, the soil cannot control water seepage, and as a result, a turbulent flow is created by increasing the discharge of water

Table 6 Details of boiling test results for the sand reinforced by geotextiles

Type of the geotextile	Relative compaction (%)	Number of layers	i_{cr}	k (cm/s)	Seepage force during sand boiling (N)
Unreinforced	80	0	0.78	0.078	6.12
	90	0	0.98	0.055	7.69
	96	0	1.5	0.03	11.77
Nonwoven	80	1	0.98	0.077	7.69
	90	1	1.77	0.038	13.89
	96	1	1.87	0.029	14.67
Woven	80	1	0.98	0.067	7.69
	90	1	1.77	0.038	13.89
	96	1	2.14	0.026	16.79
Nonwoven	80	2	1.18	0.076	9.26
	90	2	1.97	0.037	15.46
	96	2	2.27	0.029	17.81
Woven	80	2	1.18	0.061	9.26
	90	2	1.97	0.036	15.46
	96	2	2.67	0.021	20.95

Fig. 9 Variations of the critical hydraulic gradient versus relative compaction for different fiber contents (BCF)



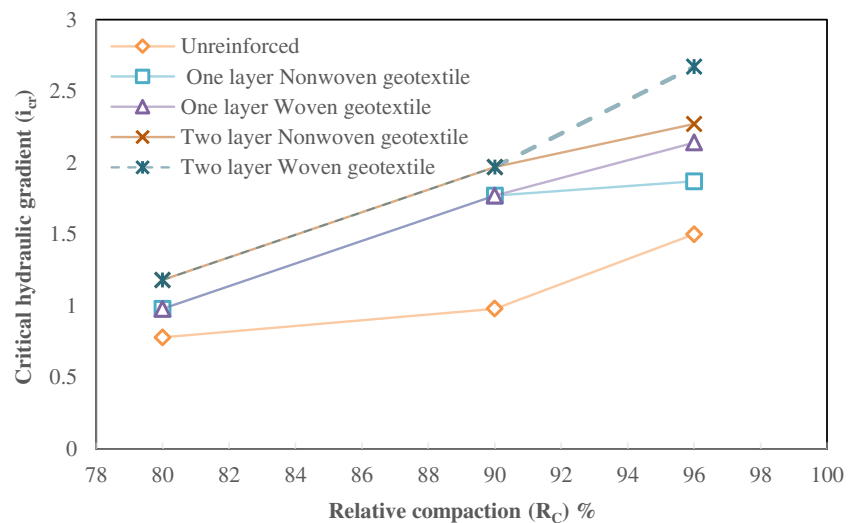
The effect of relative compaction on the results of sand boiling tests

According to Tables 5 and 6, increasing the relative compaction of the specimens (natural and reinforced with fibers and geotextiles) increases the seepage force at the moment of boiling. In fact, with increasing the relative compaction, the soil particles become closer together and the porosity of the specimens decreases, thereupon more force required for the hydraulic failure of the specimen. For natural samples, with increasing relative compaction by 16% (improvement of the loose sample and converting it to a dense sample), the required amount of the seepage force for boiling was increased from 6.12 to 11.77 (N), and this incremental trend for reinforced samples with fiber and geotextile is observed as well. The increase in relative compaction also affects the values of the critical hydraulic gradient and the permeability coefficient. Based on the obtained results in Table 5, with increasing relative compaction of the samples, the permeability coefficient has decreased

and the critical hydraulic gradient has increased. In other words, by compressing the sample, the flow is controlled and the boiling is delayed. Figure 9 shows variations of the critical hydraulic gradients versus relative compaction for reinforced specimens with BCF fiber and natural specimens.

According to Figure 9, the critical hydraulic gradient has a direct relationship with the relative compaction. In fact, with increasing the relative compaction (decreasing the porosity), the solidarity of the soil particles increases and as a result, a dense sample fails at a higher hydraulic gradient than the loose specimens. For example, in natural specimens, the values of critical soil hydraulic gradients at 80% and 96% relative compaction are 0.78 and 1.5, respectively. As can be seen, performing the compaction operations on the natural sample leads to a 100% increase in the critical hydraulic gradients. In reinforced samples with fiber, there is an incremental trend of strength against the boiling phenomenon by compaction of the sample. For example, by increasing the relative compaction

Fig. 10 Critical gradients against relative compaction for reinforced sample with geotextile



by 16% in samples reinforced with 0.5% fibers, the critical hydraulic gradient of the sample increased from 0.98 to 3.05, indicating a 200% increase in resistance to this phenomenon. In fact, as the relative compaction increases by the same amount, the resistance of the reinforced sample increases at a higher rate compared to the natural sample. Figure 10 shows the values of critical hydraulic versus relative compaction for reinforced samples by geotextiles.

According to Figure 10, increasing the relative compaction causes the improvement of the reinforced samples by a geotextile. For example, the value of critical hydraulic gradient by adding two layers of geotextiles in the loose compaction state is 1.18, while compressing the sample and increasing the relative compacting by 16%, the critical hydraulic gradient amount of the sample increases by 2.67. It can be seen in Figure 10 that in the relative compactions of 80% and 90%, the related curves to the reinforced samples with woven and nonwoven geotextiles have overlapped. Yang et al. (2017) examined the effect of polypropylene fibers on sandy soil under the piping test at relative compaction of 50% and 70% and showed that denser specimens were more resistant against boiling and occurrence of hydraulic fracture occurred at a higher hydraulic gradient.

The effect of BCF fiber percentage on critical hydraulic gradients and permeability coefficient of the sample

Figure 11 shows the variations of discharge velocity versus hydraulic gradient for reinforced samples with different percentages of the BCF fiber in compaction conditions of loose, medium compaction, and dense. According to Figure 11a, in samples with relative compaction of 80% (loose specimens), the addition of fiber increases the soil's resistance to boiling. But an increase in the weight percentage of the fiber does not affect critical hydraulic gradient. In fact, in samples with relative compaction of 80%, the critical hydraulic gradient increases to 0.98 by adding only 0.1% of the fibers, while the natural sample (without fibers) fails at 0.78 critical hydraulic gradients. On the other hand, the increase in the percentage of fibers in reinforced specimens with relative compaction of 80% has not affected the test results. In other words, for samples in the loose state and with different values of fiber mixing percentage, the critical hydraulic gradient of the sample is 0.98. Figure 12 shows the permeability coefficient variations of the samples versus the relative compaction for different mixing percentages of fiber. According to Figure 12, increasing the percentage of fibers increases the permeability coefficient in loose specimens ($R_c = 80\%$), because the void volume of soil increases in these situations. In other words, in loose specimens due to the lack of compaction of the specimen, the fibers do not mix well with the soil and there might be space between the fibers and the soil, and as a result, the velocity of water seepage increases. Figure 11c and 11b show variations

in seepage velocities in terms of hydraulic gradients for samples with relative compactions of 90% and 96% (medium and high density), respectively. Reinforced fiber specimens are more resistant to boiling than natural samples and the increase in the weight percentage of the fibers has increased the resistance of the sample to boiling. As can be seen in Figure 11b and 11c with increasing the percentage of fibers, the failure point of the graph moves to the right (greater values of critical hydraulic gradients). Also, according to Figure 12, by increasing the weight percentage of fibers for the reinforced samples with relative compactions of 90 and 96, the permeability coefficient reduces, and water seepage is controlled.

The effect of type and number of geotextiles on critical hydraulic gradients and the permeability coefficient

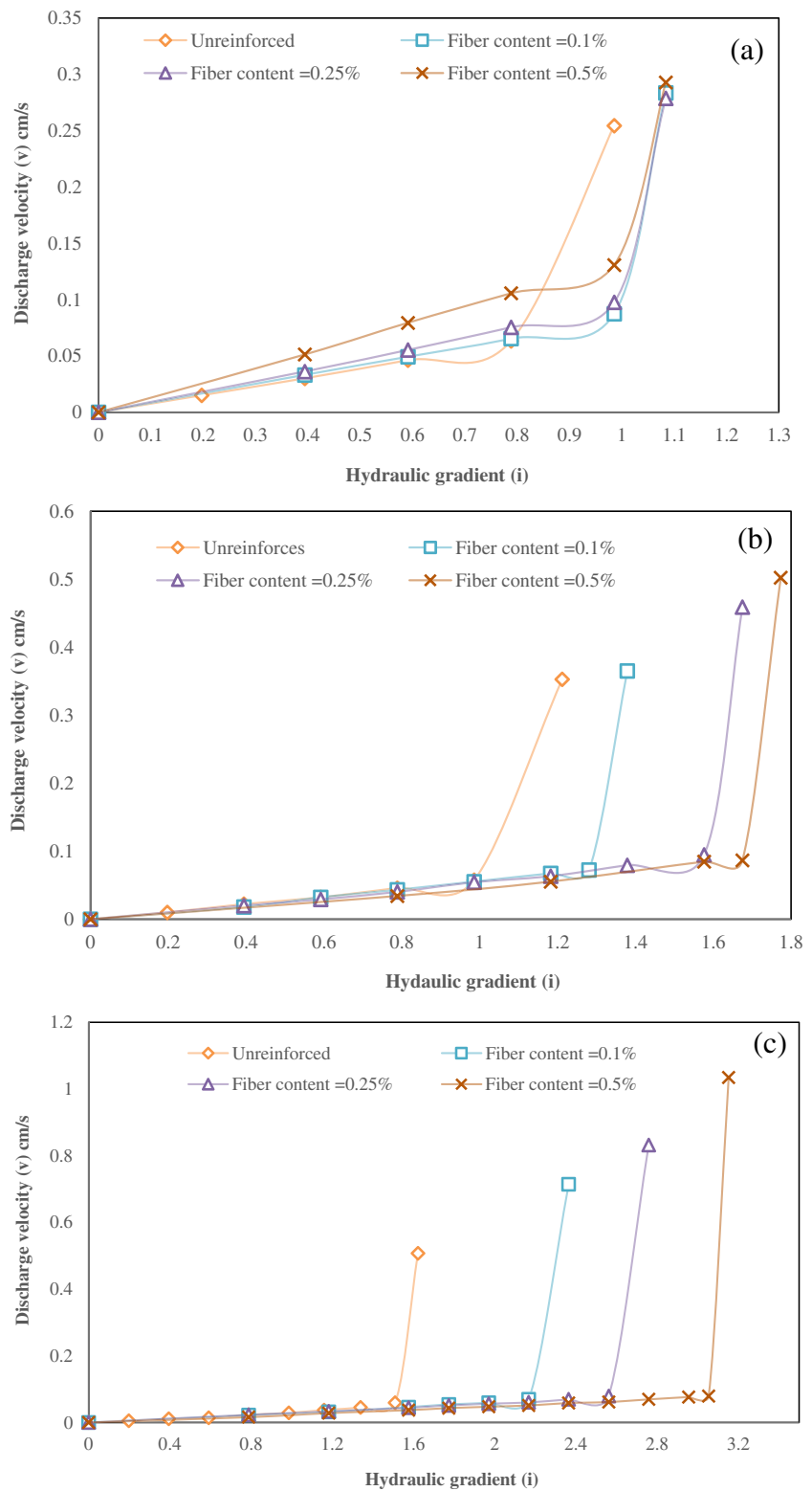
For samples with relative compaction of 80% and 90%, the geotextile type does not affect the critical hydraulic gradients of soil. According to Figure 13, in the state of loose and medium compaction, the critical hydraulic gradient is equal for similar samples (equivalent relative compaction and layer number) and reinforced with woven and nonwoven geotextile. While in $R_c = 96\%$ (dense stage), geotextile type had affected sand boiling results. Actually, according to Figure 13, at 96% relative compaction, woven geotextiles have performed better than nonwoven geotextiles. In other words, densely reinforced samples with woven geotextiles at a higher critical hydraulic gradient than similar samples but reinforced with nonwoven geotextiles are subject to boiling and as a result failure. This advantage is seen in conditions of single and double layers. But generally for reinforced samples by geotextile in all compaction conditions ($R_c = 80\%$, 90%, and 96%), increasing the number of layers increases the sample's resistance to the phenomenon of hydraulic failure, and samples with two reinforcement layers have shown more resistance to failure.

Figure 14 shows the permeability coefficients of reinforced specimens with geotextile compared to natural specimens. Woven geotextiles have better control than nonwoven geotextiles against the water seepage, as the woven geotextiles permeability is lower than that of nonwoven geotextiles. In other words, woven geotextiles due to the smaller opening size in their textile have less permeability than nonwoven geotextiles. So, in these samples (reinforced by woven geotextile), the flow rate of water was reduced significantly and, consequently, causes the seepage control.

The comparison of the results of this study with previous research

As mentioned earlier, so far, the effect of parameters such as fiber type, weight percentage, and fiber length on critical

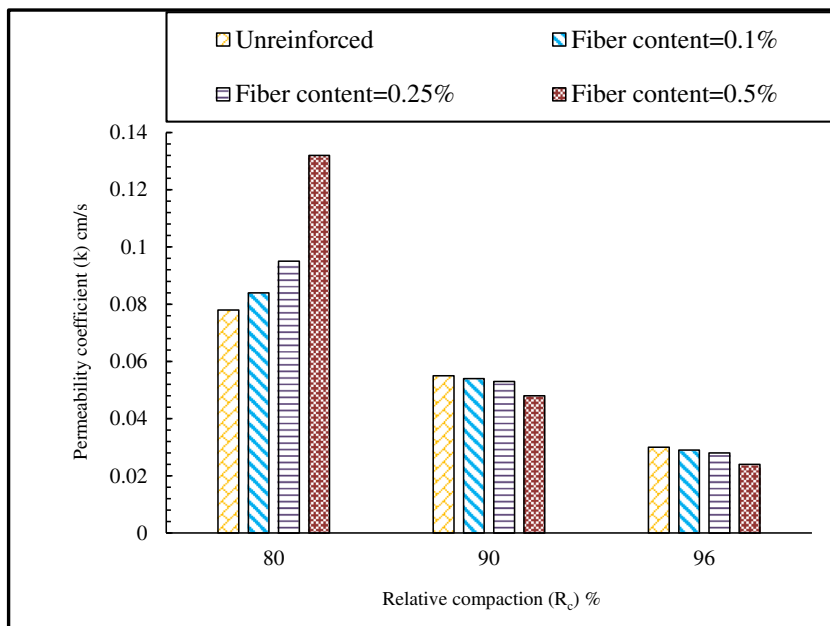
Fig. 11 Variations of discharge velocity versus hydraulic gradient for different fiber contents (a) $R_c = 80\%$, (b) $R_c = 90\%$, and (c) $R_c = 96\%$



hydraulic gradients of sandy soils has been investigated by various researchers. In Table 7, the investigation’s results of these researchers have been presented. The last column in Table 7 shows the performance of the used improvement methods (i.e., the percentage increase

in critical hydraulic gradient) by different researchers. In all of these studies, the relative compaction parameter has been considered constant, and different improvement methods have been performed in the dense state of the samples.

Fig. 12 Variations of Darcy coefficient with relative compaction for different fiber contents



According to Table 7, the most percentage of increase in soil resistance to boiling (best performance) is related to the carried-out research by Furumoto et al. (2002). In their studies, critical soil hydraulic gradient increased with 0.4% polypropylene fibers by 124.7% compared to the natural sample. In investigations of Sivakumar and Vasudevan (2008); Das et al. (2009); Das and Viswanadham (2010); Soltannejad et al. (2016); and Estabragh et al. (2016), in addition to the weight percentage of fibers, fiber length has also affected the results, so that with increasing fiber length, the critical hydraulic gradient has increased. Sivakumar and Vasudevan (2008) used natural coconut fibers to increase critical hydraulic gradients. According to their results, the sample strength increased by 36% and had a lesser effect on hydraulic failure than other fibers. However, in addition to the characteristics of the

reinforcement, the type of soil also affects the reinforcing process. In this paper, the percentage of increasing strength for reinforced soils by BCF fibers is higher than that of geotextiles, and by compressing and adding fibers to the soil, the amount of critical hydraulic gradients is increased by 291% compared to the normal sample in the loose state. This value shows the combined effect of fibers and compaction on the resistance of the sample to hydraulic failure. In fact, the effect of adding fibers to soil is 103% out of this value (291%). In other words, the strength against boiling increases by 103% by adding 0.5% BCF fiber to the sand in dens conditions. Figure 15 shows the amount of critical hydraulic gradient before and after the improvement operation in this study and other researchers' studies.

Fig. 13 The critical hydraulic gradients with relative compaction for different types of geotextile and number of geotextiles

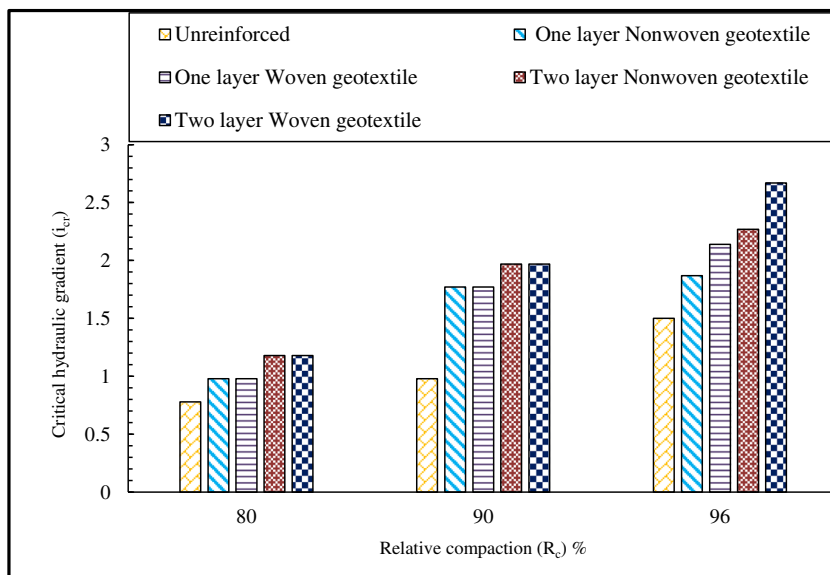
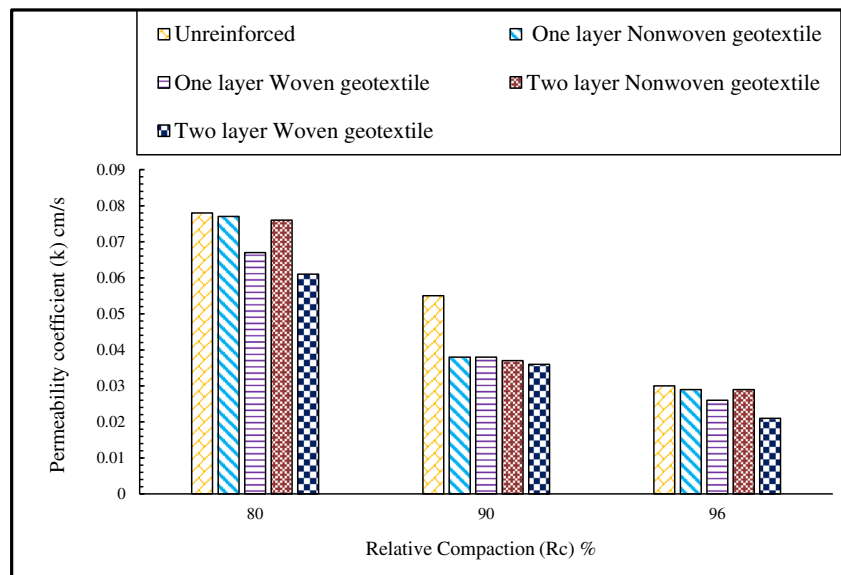


Fig. 14 Sample permeability versus relative compaction for different types of geotextile and number of geotextiles



Conclusions

This study was conducted to investigate the effect of BCF and geotextile fibers on resistance to boiling and hydraulic failure of a type of sand with boiling potential. For this purpose, an apparatus for measuring hydraulic gradient in upward flow was designed and fabricated. Several experimental tests were performed to

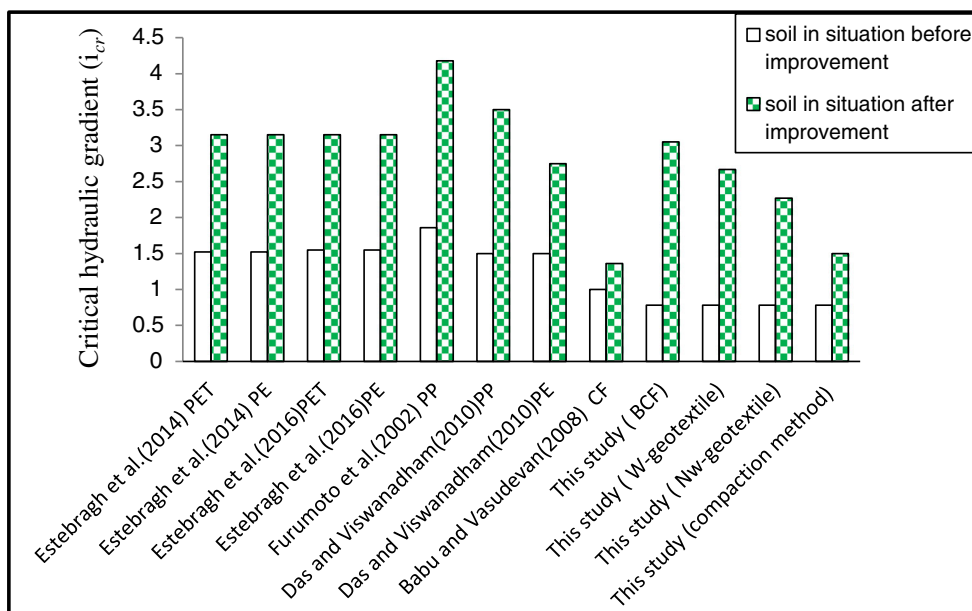
measure critical hydraulic gradients at different relative compactions of natural and reinforced specimens. Overall, 24 experiments were prepared on natural and reinforced conditions with fiber (by randomly distributed), geotextiles (as single and double layers), and the results were examined. The most important experimental results concerning sand boiling potential obtained in this research are as follows:

Table 7 Summary of reinforcement influence on the critical hydraulic gradient in the literature

Reference	Soil type (USCS)	D_r (%) ^a	Reinforcement	Variables	Number of test	Percentage of increasing i_{cr} (%)
Soltannejad et al. (2016)	SM	100	PET ^b	Content and length of fiber	17	107.2
	SM	100	PE ^c	Content and length of fiber	17	107.2
Estabragh et al. (2016)	SM	100	PET	Content and length of fiber	17	103.2
	SM	100	PE	Content and length of fiber	17	103.2
Furumoto et al. (2002)	SP	>50	PP ^d	Fiber content	4	124.7
Das and Viswanadham (2010)	SM	85	PP	Content and length of fiber	7	116
	SM	85	PE	Content and length of fiber	7	83.3
Sivakumar Babu and Vasudevan (2008)	SP	N/A	CF ^e	Fiber content	4	36
	SP	0, 50, 80	Bulk continuous filament	Fiber content and R_c	12	291
This study	SP	0, 50, 80	Woven geotextile	Layer number and R_c	9	242
	SP	0, 50, 80	Nonwoven geotextile	Layer number and R_c	9	191
	SP	0, 50, 80	Unreinforced	R_c	3	92.3

^a The relative density is estimated using $R_c = 80 + 0.2D_r$ by Lee and Singh (1971). ^b Polyethylene fiber, ^c Polyester fiber, ^d Polypropylen fiber, ^e Coconut fiber

Fig. 15 The critical hydraulic gradient before and after improvement for different references



1. Increasing the relative compaction of the samples increases the critical hydraulic gradient and consequently, the seepage force increases at the moment of boiling occurrence (the required force for hydraulic failure). In other words, dense samples with water seepage control (reducing permeability coefficient) delayed hydraulic failure.
2. In reinforcing the soil with BCF fibers, increasing the percentage of fibers increases the Darcy coefficient and, as a result, rises the discharge velocity of the output water in the reinforced sample compared to the unreinforced sample in the loose compaction state ($R_c = 80\%$). Although reinforced specimens with fibers are more resistant than natural specimens, the increase in fiber percentage does not affect the critical soil hydraulic gradients, according to the obtained results. However, the trend of critical hydraulic gradient variations in the relative compactions of 90% and 96% compared to those of 80% is different for reinforced samples with BCF fiber. In 90% and 96% relative compaction samples, the water flow velocity decreases with increasing the weight percentage of fibers, and fiber causes water seepage control inside the soil and the reinforced samples have a lower permeability coefficient than the natural sample. Also, increasing the percentage of fibers increases the critical hydraulic gradient of the soil. In other words, by adding only 0.5% BCF fibers to the compacted sand, the values of critical hydraulic gradients increase by 100% compared to the same natural sample.
3. Reinforced specimens by geotextile have a higher strength than the natural specimen at relative compaction of 80, 90, and 96%. Also, the critical hydraulic gradient of the specimens with two layers of the reinforcement element is higher than the critical hydraulic

gradient with the single layer of the reinforcement element. Increasing the number of layers increases the resistance of the sample to boiling. The important point in the relative compaction of 80 and 90% is that the type of geotextile is not affected the results of the experimental tests. In other words, the values of critical hydraulic gradients for the reinforced sample with woven and nonwoven geotextiles show the same results. While in geotextile reinforcement at relative compaction of 96%, the reinforced samples with woven geotextiles are more resistant against boiling than the ones with nonwoven geotextiles. This issue may be related to the lower permeability coefficient of the woven geotextile samples than the nonwoven geotextile ones.

4. The presence of reinforcement in the soil texture controls water seepage and by reducing the permeability coefficient of the sample, it causes a delay for the boiling phenomenon. Also using soil reinforcement such as BCF prevents hydraulic failure and causes an increase in the critical hydraulic gradient of the sample due to increased interaction between the reinforcement and the soil particles. In addition, fibers and geotextiles are environmentally friendly material which can be recycled and classified as high durability material.

Notation

Basic SI units are given in parentheses A , sample cross-section (cm^2); C_c , curvature coefficient (dimensionless); C_u , uniformity coefficient (dimensionless); D_{10} , effective particle size (mm); D_{50} , mean particle size (mm); D_r , relative density (dimensionless); F , seepage force (N); $F\%$, fiber percentage (dimensionless); G_s , specific gravity of natural soil

(dimensionless); i_{cr} , critical hydraulic gradient (dimensionless); K , permeability coefficient (cm/s); Q , discharge flow (cm³/s); R_c , relative compaction (dimensionless); Re , Reynolds number (dimensionless); V , sample volume (cm³); v , discharge velocity (cm/s); W_f , weight of fiber (g); W_T , weight of sample (g); W_s , weight of soil (g); γ_{dmax} , maximum dry unit weight (g/cm³); γ_{dmin} , minimum dry unit weight (g/cm³); γ_{sample} , dry unit weight of sample (g/cm³)

Acknowledgements The authors thank Mr. Mahdavi and Dr. Bahardoost for their valuable technical assistance and support in conducting this project.

Code availability Not applicable

Data availability The obtained data from experiments are in the “Results and discussion” section, and if you need the details of laboratory results, we can send an Excel file.

Declarations

Conflict of interest The authors declare that they have no competing interests.

References

- ASTM D4253-16e1, Standard Test Methods for Maximum Index Density and Unit Weight of Soils Using a Vibratory Table, ASTM International, West Conshohocken, PA, 2016, <https://www.astm.org/>
- ASTM D2487-17, Standard Practice for Classification of Soils for Engineering Purposes (Unified Soil Classification System), ASTM International, West Conshohocken, PA, 2017, <https://www.astm.org/>
- ASTM D4254-16, Standard Test Methods for Minimum Index Density and Unit Weight of Soils and Calculation of Relative Density, ASTM International, West Conshohocken, PA, 2016, <https://www.astm.org/>
- Azar E, Parvizi M, Rahimi H (2019) Numerical modeling of fluid sand boiling from coastal dike foundations. *Geotech Geol Eng*:1–11
- Bhagvatekshmi S, Mohan M, Sreedharan K, Ajaykumar B (2015) Evaluation of the factors controlling the spatial distribution of soil piping, a case study from the southern Western Ghats, India. *Arab J Geosci* 8(10):8055–8067
- Chegenizadeh A, Keramatikerman M, Nikraz H (2018) Liquefaction resistance of fibre reinforced low-plasticity silt. *Soil Dyn Earthq Eng* 104:372–377
- Das, B. M. (2019). *Advanced soil mechanics*. CRC press.
- Das A, Viswanadham BVS (2010) Experiments on the piping behavior of geofiber-reinforced soil. *Geosynth Int* 17(4):171–182
- Das A, Jayashree C, Viswanadham BVS (2009) Effect of randomly distributed geofibers on the piping behaviour of embankments constructed with fly ash as a fill material. *Geotext Geomembr* 27(5):341–349
- Divya PV, Viswanadham BVS, Gourc JP (2018) Hydraulic conductivity behaviour of soil blended with geofiber inclusions. *Geotext Geomembr* 46(2):121–130
- Estabragh AR, Soltani A, Javadi AA (2016) Models for predicting the seepage velocity and seepage force in a fiber reinforced silty soil. *Comput Geotech* 75:174–181
- Falamaki A, Shafiee A, Eskandari M, Mohamadzadebabr K (2020) Choice of fiber-reinforced base material to reduce internal erosion mass transport. *Arab J Geosci* 13(5):1–10
- Foster M, Fell R, Spannagle M (2000) The statistics of embankment dam failures and accidents. *Can Geotech J* 37(5):1000–1024
- Fujisawa K, Murakami A, Nishimura SI, Shuku T (2013) Relation between seepage force and velocity of sand particles during sand boiling. *Geotech Eng J SEAGS & AGSSEA* 44(2):9–17
- Furumoto K, Miki H, Tsuneoka N, Obata T (2002) Model test on the piping resistance of short fiber reinforced soil and its application to river levee. In: *Proc, 7th Int. Conf. on Geosynthetics*, Sweets & Zeitlinger, Lisse, pp 1241–1244
- Jewel A, Fujisawa K, Murakami A (2019) Effect of seepage flow on incipient motion of sand particles in a bed subjected to surface flow. *J Hydrol* 579:124178
- Lee KL, Singh A (1971) Relative density and relative compaction. *J Soil Mech Foundations Div* 97(7):1049–1052
- Liu J (1992) Seepage stability and seepage control of soil. *Water Resources and Electric Power Press, Beijing (in Chinese)*
- Richards KS, Reddy KR (2010) True triaxial piping test apparatus for evaluation of piping potential in earth structures. *Geotech Test J* 33(1):83–95
- Sellmeijer, J. B. (1988). On the mechanism of piping under impervious structures
- Sivakumar Babu GL, Vasudevan AK (2008) Seepage velocity and piping resistance of coir fiber mixed soils. *J Irrig Drain Eng* 134(4):485–492
- Skempton AW, Brogan JM (1994) Experiments on piping in sandy gravels. *Geotechnique* 44(3):449–460
- Soltannejad KHALED, Estabragh AR, Hamid M, Abdolahi J (2016) Effect of randomly reinforced soil on increasing resistance against piping phenomenon. *Amirkabir J Civil Eng* 48(4):429–438
- Taghvaei P, Mousavi SF, Shahnazari A, Karami H, Shoshpash I (2019) Experimental and numerical modeling of nano-clay effect on seepage rate in earth dams. *Int J Geosynthetics Ground Eng* 5(1):1
- Terzaghi, K. (1943). Theoretical soil mechanics. John Wiley & sons. *New York*, 11–15
- Tian D, Xie Q, Fu X, Zhang J (2020) Experimental study on the effect of fine contents on internal erosion in natural soil deposits. *Bull Eng Geol Environ* 79:4135–4150
- Van Beek VM, De Bruijn HTJ, Knoeff JG, Bezuijen A, Förster U (2010) Levee failure due to piping: A full-scale experiment. In *Scour and Erosion* 283–292
- Wu LJ (1980) Calculation of critical hydraulic gradient for piping in cohesionless soils. *Hydro-Sci Eng* 4:90–95
- Yang KH, Wang JY (2017) Experiment and statistical assessment on piping failures in soils with different gradations. *Mar Georesour Geotechnol* 35(4):512–527
- Yang KH, Adilehou WM, Jian ST, Wei SB (2017) Hydraulic response of fibre-reinforced sand subject to seepage. *Geosynth Int* 24(5):491–507
- Yang Y, Wei Z, Cao G, Yang Y, Wang H, Zhuang S, Lu T (2019) A case study on utilizing geotextile tubes for tailings dams construction in China. *Geotext Geomembr* 47(2):187–192
- Yetimoglu T, Salbas O (2003) A study on shear strength of sands reinforced with randomly distributed discrete fibers. *Geotext Geomembr* 21(2):103–110
- Zhou J, Bai YF, Yao ZX (2010) A mathematical model for determination of the critical hydraulic gradient in soil piping. In *Geoenvironmental Engineering and Geotechnics: Progress in Modeling and Applications* 239–244